



OPEN

SUBJECT AREAS:

GLASSES

OPTICAL MATERIALS AND
STRUCTURESReceived
2 April 2014Accepted
22 May 2014Published
11 June 2014

Correspondence and
requests for materials
should be addressed to
L.Z. (lzhang@siom.ac.
cn) or X.Y.
(xiangqiang@siom.ac.
cn)

The effect of La_2O_3 in Tm^{3+} -doped germanate-tellurite glasses for $\sim 2 \mu\text{m}$ emission

Ya-Pei Peng^{1,2}, Xinqiang Yuan¹, Junjie Zhang³ & Long Zhang¹

¹Key Laboratory of Materials for High Power Laser, Shanghai Institute of Optics and Fine Mechanics, Chinese Academy of Sciences, Shanghai 201800, China, ²University of Chinese Academy of Sciences, Beijing 100039, China, ³College of Materials Science and Engineering, China Jiliang University, Zhejiang 310018, China.

A germanate-tellurite glass ($\text{GeO}_2\text{-TeO}_2\text{-K}_2\text{O-Nb}_2\text{O}_5\text{-La}_2\text{O}_3$) with thulium doping has been investigated for application as a laser material around $2.0 \mu\text{m}$ regions. Under the 808 nm laser diode pumped, intense $1.8 \mu\text{m}$ emission is obtained. Based on the absorption spectra, radiative properties are predicted using Judd-Ofelt theory. The maximum value of emission cross-section of Tm^{3+} around $1.8 \mu\text{m}$ can reach $1.46 \times 10^{-20} \text{ cm}^2$, which indicated that the germanate-tellurite glass may provide high gain as a good medium for efficient $1.8 \mu\text{m}$ laser system.

Recently, Tm^{3+} doped glass has been widely investigated for mid-infrared fiber lasers around $2.0 \mu\text{m}$ since the transitions of $\text{Tm}^{3+}:^3\text{F}_4 \rightarrow ^3\text{H}_6$. The mid-infrared fiber lasers in the $2.0 \mu\text{m}$ have generated great interest for its potential applications in several fields, such as medical surgery, remote sensing, eye-safe laser radar, military, and atmospheric pollution monitoring in the last decades¹⁻⁴. Rare-earth thulium ions are often chosen to produce laser radiation at $1.8 \mu\text{m}$ through the transitions of $\text{Tm}^{3+}:^3\text{F}_4 \rightarrow ^3\text{H}_6$. In this paper, Tm^{3+} has been selected as active ions because the ground state of $\text{Tm}^{3+}:^3\text{H}_6$ can be pumped directly by 808 nm commercial laser diodes. Laser emission at $1.8 \mu\text{m}$ strongly depends on the efficiency of the energy transfer process among Tm^{3+} ions. In order to obtain high-power infrared emissions from Tm^{3+} , the host glass plays an important role. Most researches in Tm^{3+} doped glass matrix for $\sim 2.0 \mu\text{m}$ emission have focused on silica⁵⁻⁸, silicate⁹⁻¹¹, fluoride¹²⁻¹⁴, fluorophosphates¹⁵⁻¹⁷, tellurite¹⁸⁻²¹, and germanate²²⁻²⁵ based glasses. Due to the energy cross-relaxation process, the host material should be chosen to have high solubility of the thulium ions. Compared with SiO_2 -based glass, $\text{GeO}_2\text{-TeO}_2$ -based glass have the higher solubility for Tm^{3+} ions and the lower phonon energy (germanate-tellurite glass' is about $800\text{-}900 \text{ cm}^{-1}$), which can avoid very competitive nonradiative decay for Tm^{3+} ions. High phonon energy leads to faster multi-phonon relaxation and thus results in lower cross-relaxation rate. By contrast with germanate-tellurite glass, fluoride glass also has very low phonon energy (around 500 cm^{-1}) but the low mechanical strength and damage threshold limit its application in high power or energy fiber laser systems. Therefore, germanate-tellurite glass may have higher ions solubility and appropriate phonon energy for developing more efficient optical devices by comprehensive evaluation.

In this work, we report primarily a series of glass compositions in the Tm^{3+} -doped germanate-tellurite (GT) glasses to study mid-infrared spectroscopic properties. We induce La_2O_3 to substitute for Nb_2O_5 to improve the thermal stability and anti-crystallization of this glass system, by reasons of the ratio of La^{3+} ions (0.12 nm) and coordination number (8) are higher than Nb^{5+} ions (ratio = $0.07 \text{ nm}/\text{coordination number} = 6$). The absorption and emission spectra of Tm^{3+} -doped GT glasses were obtained. Results and analysis reveal that these germanate-tellurite glasses with good spectroscopic properties may provide a high gain as a good medium for high-power level laser.

Experiments and measurements

The germanate-tellurite glass with molar composition of $70\text{GeO}_2\text{-}10\text{TeO}_2\text{-}10\text{K}_2\text{O}\text{-}(9\text{-}x)\text{Nb}_2\text{O}_5\text{-}x\text{La}_2\text{O}_3\text{-}1\text{Tm}_2\text{O}_3$ ($x = 1, 3, 5, \text{ and } 7 \text{ mol. \%}$) was investigated, which is hereafter denoted as GTLa-x glass. All the samples were prepared by traditional melt-quenching method with using high-purity of GeO_2 , TeO_2 , K_2CO_3 , Nb_2O_5 , La_2O_3 , and Tm_2O_3 powder. Well-mixed 20 g batches of the samples were placed in a platinum crucible and heated with a SiC-resistance electric furnace at 1150°C for 30 min to melt. The melt was poured onto a preheated steel plate and



annealed for 2 hours in a furnace around the glass transition temperature (T_g), after which it was allowed to cool slowly in the furnace to room temperature. The annealed samples were fabricated and polished to $10 \times 10 \times 1$ mm for optical measurements.

The density was tested by Archimedes' liquid-immersion method in distilled water and the refractive index of the glass samples was measured by prism minimum deviation method. The DSC curve is recorded by NETZSCH STA 409PC. Furthermore, the absorption spectra were recorded with a Perkin-Elmer-Lambda 900 UV/VIS/NIR spectrophotometer in the range of 300–2000 nm, and the emission spectra were measured with a Triax 320 type spectrometer (Jobin-Yvon Co., France) upon excitation at 808 nm. For the fluorescence lifetime measurements, the instrument applied was FLSP 920 fluorescence spectrophotometer (Edinburgh Analytical Instruments Ltd, UK). All the measurements were carried out at room temperature.

Results and discussion

Thermal property. Figure 1 shows the thermal property of GTLa-x glass from 300 °C to 900 °C. From the DSC curve of present glasses system, we can find out that no crystallization peak is apparent, and the glass transition temperature T_g are 355 °C, 459 °C, 550 °C, respectively. The T_g increase with the contents of La_2O_3 increase. It indicated the introduce La_2O_3 to substitute for Nb_2O_5 can improve the thermal stability and anti-crystallization ability of this glass system. We could conclude that thermal properties of the GTLa-x glass are good for fiber drawing from the analysis of DSC curve.

Absorption spectrum. The absorption spectra were obtained at room temperature over a wavelength region of 300–2000 nm. The absorption spectra of the GTLa-x samples at room temperature is shown in Fig. 2, and the absorption bands centered corresponding to the transitions from the $^3\text{H}_6$ ground state to the excited state of $^3\text{F}_4$ (1694 nm), $^3\text{H}_5$ (1208 nm), $^3\text{H}_4$ (792 nm), $^3\text{F}_2 + ^3\text{F}_3$ (686 nm) and $^1\text{G}_4$ (492 nm), respectively. The transitions to energy levels higher than $^1\text{G}_4$ are not observed because of the intrinsic band gap absorption of host glass. The insert of the figure 2 is the transmittance curve of the GTLa-3 glass sample from 2.5 μm to 8 μm . We can find that the OH^- concentration on present glass sample is larger and result in the larger absorption around 3 μm regions. As well known, OH^- groups play an important role and the much OH^- groups on glass host would decrease the performance of the 1.8 μm emission. So, improving the OH^- concentration on present glass system is a crucial issue to obtain efficiently 1.8 μm emission.

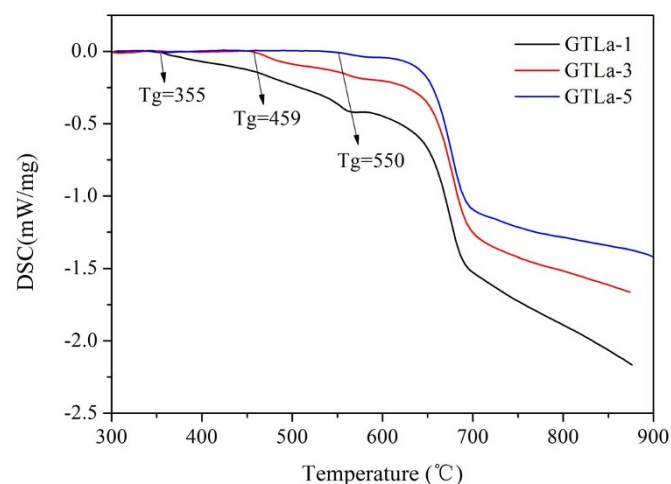


Figure 1 | DSC curve of GTLa-x glasses.

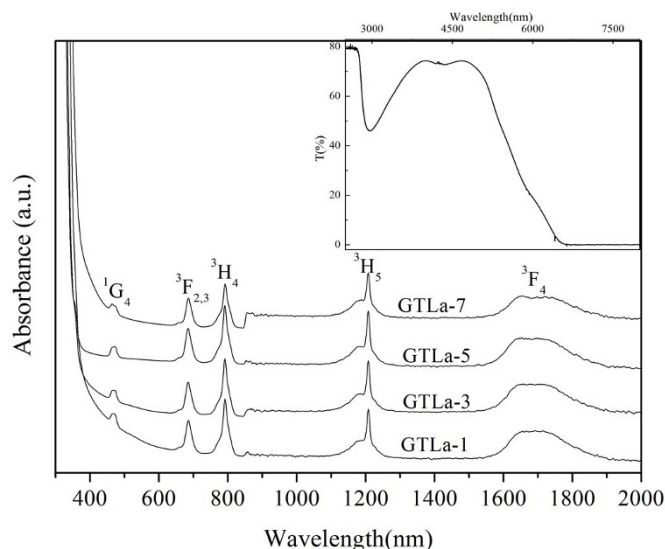


Figure 2 | Absorption spectra of GT glasses. The insert of figure is the transmittance curve of GTLa-3.

Judd-Ofelt analysis. Judd-Ofelt (J-O) theory^{26,27} has been commonly applied to determine the important spectroscopic and laser parameters of rare earth ions doped glasses by many researchers. According to the J-O theory, based on absorption spectra, the measured oscillator strengths and some spectroscopic parameters of many trivalent rare earths in solids, such as intensity parameters Ω_λ , radiative transition probability A_{rad} , and radiative lifetime τ_{rad} can be calculated. The theoretical (f_{theor}) and the measured (f_{exp}) oscillator strengths of the GTLa-1 glass are shown in Table 1.

As is shown in Table 1, the root-mean-square error deviation of intensity parameters is 0.39×10^{-6} , which indicates the validity of the J-O theory for predicting the spectral intensities of Tm^{3+} and the reliable calculation. The J-O intensity parameters are important for investigating the local structure and bonding in the vicinity of RE ions. As known large Ω_2 parameter is related with the amount of the strong covalent bond between rare-earth ions and ligand anions, strongly depends on the asymmetry of the local environment at the Tm^{3+} ion site in the glass hosts, and a strong polarizability of the anion, while the Ω_6 parameter is related to the overlap integrals of $4f$ and $5d$ orbitals^{28,29}. Values of Ω_4 and Ω_6 also provide some information on the rigidity and viscosity of hosts³⁰. In this work, the J-O intensity parameters Ω_λ are compared with those of various Tm^{3+} doped glasses presented in Table 2. It can be found that the value of Ω_2 becomes small when La_2O_3 increase but $\text{La}_2\text{O}_3 < \text{Nb}_2\text{O}_5$. When the contents of La_2O_3 approximate that of Nb_2O_5 , the value of Ω_2 increases slightly, while $\text{La}_2\text{O}_3 > \text{Nb}_2\text{O}_5$, the value of Ω_2 drop down quickly. Similarly, Ω_6 also changed with the contents of La_2O_3 . These proved the change of asymmetry of the local environment at the Tm^{3+} ion site and found a variation in the covalent and bond strength of Tm-O in glass hosts. In table 2, Ω_2 for GTLa-x glass is

Table 1 | Measured and calculated oscillator strengths of Tm^{3+} in GTLa-1 glass

Absorption	λ (nm)	$ \langle U^{(2)} \rangle ^2$	$ \langle U^{(4)} \rangle ^2$	$ \langle U^{(6)} \rangle ^2$	Oscillator strength (10^{-6})	
					Measured	Calculated
$^3\text{H}_6 \rightarrow ^3\text{F}_4$	1694	0.5470	0.7355	0.2462	3.531	3.529
$^3\text{H}_6 \rightarrow ^3\text{H}_4$	792	0.2300	0.1032	0.5880	3.836	3.844
$^3\text{H}_6 \rightarrow ^3\text{F}_3$	686	0	0.3162	0.8408	2.796	2.819
$^3\text{H}_6 \rightarrow ^1\text{G}_4$	472	0.0006	0.0355	0.2082	1.287	0.889



Glass	Ω_2	Ω_4	Ω_6	Reference
GTLA-1	5.97	1.10	1.27	This work
GTLA-3	5.64	0.97	1.26	
GTLA-5	5.87	1.03	1.39	
GTLA-7	3.93	0.5	1.1	
Silica	3.7	2.3	0.6	[32]
Fluorophosphate	3.01	2.56	1.54	[16]
Tellurite	3.20	2.01	1.83	[19]

higher than fluoride glasses', because the electronegativity of oxide is smaller than that of fluorine. It means the asymmetry and covalent environment of the Tm-O band in GT glass are stronger than other host glasses'.

The radiative transition probabilities for $\text{Tm}^{3+}: {}^3\text{F}_4 \rightarrow {}^3\text{H}_6$ level can be calculated by using J-O intensity parameters. The results of J-O analysis are shown in Table 3. The radiative transition probability A_{rad} for the transition in GTLa-1 glass is 372.1 s^{-1} , and this value is slightly higher than those in fluorophosphate glass¹⁶. Because radiative transition probability depends intensively on the refractive indices, obtaining of larger radiative transition probability is reasonable in GT glass with higher refractive index³¹, and larger values are beneficial in achieving intense near-infrared emission.

Infrared fluorescence spectra. The fluorescence spectra of the samples are measured as shown in figure 3 to investigate the near-infrared emission characteristics of the prepared Tm^{3+} -doped GT glasses as a function of the La_2O_3 contents. Besides, the inset of figure 3 is the energy level diagram and energy transfer sketch map of Tm^{3+} when pumped at 808 nm. The cross relaxation (CR) and energy migration (EM) into the ${}^3\text{H}_4$ level are also indicated. The ${}^3\text{F}_4 \rightarrow {}^3\text{H}_6$ fluorescence around $1.8 \mu\text{m}$ is obviously observed, and the intensity is much larger than that of $1.47 \mu\text{m}$ corresponding to ${}^3\text{H}_4 \rightarrow {}^3\text{F}_4$ transition for samples under the 808 nm diode laser. The emission at $1.47 \mu\text{m}$ due to the ${}^3\text{H}_4 \rightarrow {}^3\text{F}_4$ transition is much lower in intensity relative to the $1.8 \mu\text{m}$ because the cross relaxation between Tm^{3+} ions is efficiency. Moreover, the intensity of $1.8 \mu\text{m}$ emission firstly decreased and then increased with the increment of La_2O_3 concentration. But the intensity of $1.8 \mu\text{m}$ emission slightly increased when the concentration of La_2O_3 more than the concentration of Nb_2O_5 . The maximum fluorescence peak intensity for GT glass is observed around 1 mol. % La_2O_3 .

Absorption and stimulated emission cross section. According to the absorption spectra, the absorption cross-section (σ_{abs}) can be calculated by using Beer-Lambert equation

$$\sigma_{abs}(\lambda) = \frac{\ln[I_0(\lambda)/I(\lambda)]}{Nl} \quad (1)$$

where N is the rare-earth ion concentration (ions/ cm^3), l is the sample thickness, $I_0(\lambda)$ is the incident optical intensity, and $I(\lambda)$ is the optical intensity throughout the sample.

Table 3 | The electric (S_{ed}) and magnetic (S_{md}) dipole line strengths, radiative transition probability (A_{rad}), branching ratio (β), and radiative lifetime (τ_{rad}) of Tm^{3+} in GT glass

Glass	S _L J	S' _L J'	S _{dip}		A_{rad} (s^{-1})	β (%)	τ_{rad} (ms)
			S_{ed}	S_{md}			
GTLa-1	${}^3\text{F}_4$	${}^3\text{H}_6$	44.84	0	372.1	100	2.68
GTLa-3			42.0	0	348.5	100	2.86
GTLa-5			44.07	0	365.6	100	2.73
GTLa-7			28.53	0	236.7	100	4.22

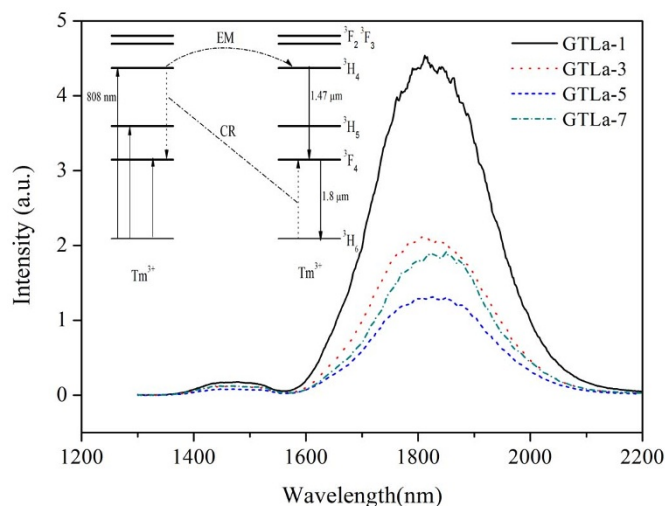


Figure 3 | Fluorescence spectra of the GT glasses with Tm^{3+} ions. The inset is the energy level diagram and energy transfer sketch map of Tm^{3+} when pumped at 808 nm.

The stimulated emission cross-section (σ_{em}) is calculated from the absorption cross-section by using McCumber formula equation³³

$$\sigma_{em}(\lambda) = \sigma_{abs}(\lambda) \frac{Z_l}{Z_u} \exp\left[\frac{hc}{kT} \left(\frac{1}{\lambda_{ZL}} - \frac{1}{\lambda}\right)\right] \quad (2)$$

where Z_l and Z_u are the partition functions of the lower and upper states, respectively, k is the Boltzmann constant, T is the temperature, and λ_{ZL} is the wavelength for the transition between the lower Stark sublevels of the emitting multiplets and the lower Stark sublevels of the receiving multiplets (so called 'zero-phonon line'). In the following calculation, the ratio of the partition functions of the lower to the upper state Z_l and Z_u is equal to 13/9, for the reason that the values of the lower and upper states Z_l and Z_u simply become the degeneracy weightings of the two states in the high temperature limit. The zero-phonon line is assumed to the peak wavelength of the absorption, $\lambda_{ZL} = \lambda_{peak-abs}$.

Figure 4 shows the σ_{abs} and σ_{em} for optical transitions involving the ground and first excited states of Tm^{3+} ions of GTLa-1 glass. The calculated maximum σ_{abs} and σ_{em} for Tm^{3+} are $4.17 \times 10^{-21} \text{ cm}^2$ at 1700 nm and $14.6 \times 10^{-21} \text{ cm}^2$ at 1806 nm, respectively. Moreover, the product of the stimulated emission cross-section and the radiative lifetime (τ_{rad}), $\sigma_{em} \times \tau_{rad}$ is another important parameter to

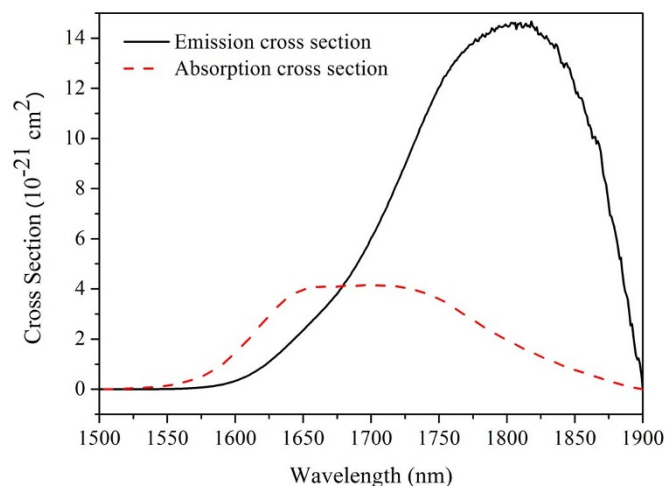


Figure 4 | The absorption and emission cross sections of GTLa-1 glass.



Table 4 | Calculated emission cross-section σ_{em} , radiative lifetime τ_{rad} , and $\sigma_{em} \times \tau_{rad}$ of ${}^3F_4 \rightarrow {}^3H_6$ transition of different Tm^{3+} -doped host glasses

Glass	σ_{em} ($\times 10^{-21}$ cm ²)	τ_{rad} (ms)	$\sigma_{em} \times \tau_{rad}$ ($\times 10^{-21}$ cm ² ms)	Reference
GTLa-1	13.56	2.68	36.3	This work
GTLa-3	14.61	2.86	41.78	
GTLa-5	13.01	2.73	35.51	
GTLa-7	8.47	4.22	35.74	
Silica	4.3	7.0	30.1	[32]
Fluorophosphate	4.11	4.44	18.2	[16]
Tellurite	9.2	1.78	16.37	[21]
Germanate	9.3	2.48	23.1	[37]

characterize laser materials, which is the figure of merit (FOM) for amplifier gain^{28,34,35}.

Table 4 shows the emission cross-section, radiative lifetime, and FOM gain ($\sigma_{em} \times \tau_{rad}$) of ${}^3F_4 \rightarrow {}^3H_6$ transition of Tm^{3+} -doped glasses. For laser glasses, it is generally desirable for the emission cross section to be as large as possible to provide a high gain³⁶. This peak emission cross section had reported as 4.3×10^{-21} cm² in silica glass by Turri³², 4.11×10^{-21} cm² in fluorophosphate by Tian¹⁶, and 9.20×10^{-21} cm² in tellurite by Balda²¹. It can be seen that the σ_{em} in GTLa-1 sample has a maximum value which is higher than that of Tm^{3+} -doped other kinds of glasses. And the $\sigma_{em} \times \tau_{rad}$ of Tm^{3+} doped GT glasses is much larger than other Tm^{3+} -doped host glasses. The advantage of GT glass possessing larger emission cross section may prove it to be a promising laser glass with high gain to scale a high power level laser.

Fluorescence lifetime. The fluorescence lifetime of $Tm^{3+}:{}^3F_4$ becomes shorter with increasing of the La_2O_3 concentrations, and the lifetime becomes longer when doped with 7 mol% La_2O_3 , as shown in table 5. However, it indicated that the measured lifetime is much shorter than the calculated lifetime. It is due to nonradiative quenching⁹. The nonradiative decay originated from several mechanisms, such as energy transfer processes between the Tm^{3+} ions themselves, multiphonon decay, etc. Energy transfer processes between the Tm^{3+} ions themselves are cross-relaxation and energy migration. The cross relaxation energy transfer process between Tm^{3+} ions described in the introduction does not quench fluorescence by itself, but energy migration is a resonant nonradiative mechanism, which increases the probability of luminescence quenching by impurities. Generally, the relatively longer radiation lifetime is beneficial to reduce the laser oscillation threshold³⁸. Therefore, this Tm^{3+} -doped GT glass can be considered as an appropriate medium to achieve a 1.8 μm laser with high quality.

Summary

Spectroscopic properties of 1.8 μm emission have been investigated in the Tm^{3+} -doped germanate-tellurite glasses (GeO_2 - TeO_2 - K_2O - Nb_2O_5 - La_2O_3). We investigate the effect of the spectroscopic properties for different compositions with varying Nb^{5+}/La^{3+} ions ratio. On the basis of our experimental results, Judd–Ofelt intensity parameter, spontaneous transition probability, radiative lifetime, and absorption cross-section, as well as stimulated emission cross-section

Table 5 | Measured fluorescence lifetime of the $Tm: {}^3H_4$ level and $Tm: {}^3F_4$ level at 295 K of different Tm^{3+} -doped host glasses

Level	GTLa-1	GTLa-3	GTLa-5	GTLa-7
$Tm^{3+}:{}^3F_4$	428.64 μs	284.40 μs	282.43 μs	482.13 μs
$Tm^{3+}:{}^3H_4$	121.42 μs	107.91 μs	110.56 μs	125.83 μs

are calculated and discussed. For the Tm^{3+} -doped GT glass samples, the fluorescence measurement shows that the maximum value of 1.8 μm emission intensity occurs in GTLa-1 glass. The optimal concentration of La_2O_3 for a laser application has been determined, which is 1 mol.% La_2O_3 . Results indicate that these germanate-tellurite glasses with good spectroscopic properties may provide a high gain as a good medium for mid-infrared laser.

- Cornacchia, F., Toncelli, A. & Tonelli, M. 2 μm lasers with fluoride crystals: Research and development. *Prog. Quant. Electron.* **33**, 61–109 (2009).
- Jackson, S. D. & Mossman, S. High-power diode-cladding-pumped Tm^{3+} , Ho^{3+} -doped silica fibre laser. *Appl. Phys. B* **77**, 489–491 (2003).
- Tsang, Y. H., Coleman, D. J. & King, T. A. High power 1.9 μm Tm^{3+} -silica fibre laser pumped at 1.09 μm by a Yb^{3+} -silica fibre laser. *Opt. Commun.* **231**, 357–364 (2004).
- de Sousa, D. F. *et al.* On the observation of 2.8 μm emission from diode-pumped Er^{3+} - and Yb^{3+} -doped low silica calcium aluminate glasses. *Appl. Phys. Lett.* **74**, 908–910 (1999).
- Tang, Y. L., Li, F. & Xu, J. Q. Short-pulse-width self-pulsed Tm^{3+} -doped silica fiber lasers. *J. Opt. Soc. Amer. B* **28**, 1051–1054 (2011).
- Hübner, P., Kieleck, C., Jackson, S. D. & Eichhorn, M. High-power actively mode-locked sub-nanosecond Tm^{3+} -doped silica fiber laser. *Opt. Lett.* **36**, 2483–2485 (2011).
- Eichhorn, M. & Jackson, S. D. High-pulse-energy actively Q-switched Tm^{3+} -doped silica 2 μm fiber laser pumped at 792 nm. *Opt. Lett.* **32**, 2780–2782 (2007).
- Frith, G., Lancaster, D. G. & Jackson, S. D. 85 W Tm^{3+} -doped silica fiber laser. *Electron. Lett.* **41**, 687–688 (2005).
- Li, M. *et al.* Investigation on Tm^{3+} -doped silicate glass for 1.8 μm emission. *J. Lumin.* **132**, 1830–1835 (2012).
- Wang, Q., Geng, J., Luo, T. & Jiang, S. Mode-locked 2 μm laser with highly thulium-doped silicate fiber. *Opt. Lett.* **34**, 3616–3618 (2009).
- Geng, J. *et al.* Single-frequency narrow-linewidth Tm -doped fiber laser using silicate glass fiber. *Opt. Lett.* **34**, 3493–3495 (2009).
- Eichhorn, M. High-gain Tm -doped fluoride fiber amplifier. *Opt. Lett.* **30**, 456–458 (2005).
- Walsh, B. M. & Barnes, N. P. Comparison of $Tm:ZBLAN$ and $Tm:silica$ fiber lasers; Spectroscopy and tunable pulsed laser operation around 1.9 μm . *Appl. Phys. B* **78**, 325–333 (2004).
- Doualan, J. L. *et al.* Spectroscopic properties and laser emission of Tm doped ZBLAN glass at 1.8 μm . *Opt. Mater.* **24**, 563–574 (2003).
- Tian, Y., Xu, R., Hu, L. & Zhang, J. Intense 2.0 μm emission properties and energy transfer of $Ho^{3+}/Tm^{3+}/Yb^{3+}$ doped fluorophosphate glasses. *J. Appl. Phys.* **110**, 033502-1-6 (2011).
- Tian, Y. *et al.* 1.8 μm emission of highly thulium doped fluorophosphate glasses. *J. Appl. Phys.* **108**, 083504-1-7 (2010).
- Wang, M. *et al.* 2 μm emission performance in Ho^{3+} doped fluorophosphate glasses sensitized with Er^{3+} and Tm^{3+} under 800 nm excitation. *Solid State Commun.* **149**, 1216–1220 (2009).
- Gomes, L. r. *et al.* Energy transfer and energy level decay processes in Tm^{3+} -doped tellurite glass. *J. Appl. Phys.* **111**, 063105-1-8 (2012).
- Xu, R., Tian, Y., Hu, L. & Zhang, J. 2 μm spectroscopic investigation of Tm^{3+} -doped tellurite glass fiber. *J. Non-Crystal. Solids* **357**, 2489–2493 (2011).
- Richards, B. *et al.* Tellurite glass lasers operating close to 2 μm . *Laser Phys. Lett.* **7**, 177–193 (2010).
- Balda, R., Fernández, J., García-Revilla, S. & Fernández-Navarro, J. M. Spectroscopy and concentration quenching of the infrared emissions in Tm^{3+} -doped TeO_2 - TiO_2 - Nb_2O_5 glass. *Opt. Express* **15**, 6750–6761 (2007).
- Shi, W. *et al.* 220 μJ monolithic single-frequency Q-switched fiber laser at 2 μm by using highly Tm -doped germanate fibers. *Opt. Lett.* **36**, 3575–3577 (2011).
- Xu, R., Tian, Y., Hu, L. & Zhang, J. Structural Origin and Energy Transfer Processes of 1.8 μm Emission in Tm^{3+} Doped Germanate Glasses. *J. Phys. Chem. A* **115**, 6488–6492 (2011).
- Shi, W. *et al.* 220 μJ Monolithic Single Frequency Actively Q-Switched 2 μm Fiber Laser by using highly Tm -doped germanate fiber. *Optics Lett.* **36**, 3575–3577 (2011).
- Xu, R., Tian, Y., Hu, L. & Zhang, J. Broadband 2 μm emission and energy-transfer properties of thulium-doped oxyfluoride germanate glass fiber. *Appl. Phys. B* **104**, 839–844 (2011).
- Judd, B. Optical Absorption Intensities of Rare-Earth Ions. *Phys. Rev.* **127**, 750–761 (1962).
- Ofelt, G. S. Intensities of Crystal Spectra of Rare-Earth Ions. *J. Chem. Phys.* **37**, 511–520 (1962).
- Heo, J., Shin, Y. B. & Jang, J. N. Spectroscopic analysis of Tm^{3+} in PbO - Bi_2O_3 - Ga_2O_3 glass. *Appl. Opt.* **34**, 4284–4289 (1995).
- Jayasimhadri, M. *et al.* Spectroscopic properties and Judd–Ofelt analysis of Sm^{3+} -doped lead–germanate–tellurite glasses. *J. Phys. D* **41**, 175101-1-7 (2008).
- Wang, X. *et al.* Spectroscopic properties of thulium ions in bismuth silicate glass. *Chin. Opt. Lett.* **10**, 101601–101605 (2012).



31. Balda, R. *et al.* Spectroscopic properties of the 1.4 μm emission of Tm^{3+} ions in $\text{TeO}_2\text{-WO}_3\text{-PbO}$ glasses. *Opt. Express* **16**, 11836–11846 (2008).
32. Turri, G. *et al.* Temperature-dependent spectroscopic properties of Tm^{3+} in germanate, silica, and phosphate glasses: A comparative study. *J. Appl. Phys.* **103**, 0931041-7- (2008).
33. McCumber, D. Theory of Phonon-Terminated Optical Masers. *Phys. Rev.* **134**, A299–A306 (1964).
34. Zou, X. & Toratani, H. Spectroscopic properties and energy transfers in Tm^{3+} singly- and $\text{Tm}^{3+}/\text{Ho}^{3+}$ doubly-doped glasses. *J. Non-Crystal. Solids* **195**(1), 113–124 (1996).
35. Fan, H. *et al.* Tm^{3+} doped $\text{Bi}_2\text{O}_3\text{-GeO}_2\text{-Na}_2\text{O}$ glasses for 1.8 μm fluorescence. *Opt. Mater.* **32**, 627–631 (2010).
36. Xu, R., Pan, J., Hu, L. & Zhang, J. 2.0 μm emission properties and energy transfer processes of $\text{Yb}^{3+}/\text{Ho}^{3+}$ codoped germanate glass. *J. Appl. Phys.* **108**, 043522-1-7 (2010).
37. Xu, R. *et al.* Spectroscopic properties of 1.8 μm emission of thulium ions in germanate glass. *Appl. Phys. B* **102**, 109–116 (2011).
38. Zhang, Q. *et al.* Spectroscopic properties of $\text{Ho}^{3+}/\text{Yb}^{3+}$ codoped lanthanum aluminum germanate glasses with efficient energy transfer. *J. Appl. Phys.* **106**, 113102-1-5 (2009).

Acknowledgments

This work is financially supported by National Natural Science Foundation of China (No. 51172252 and 51102253).

Author contributions

Y.P. wrote the main manuscript text and coauthor, X.Y. checked up. J.Z. and L.Z. are responsible for the experiment. All authors reviewed the manuscript.

Additional information

Competing financial interests: The authors declare no competing financial interests.

How to cite this article: Peng, Y.-P., Yuan, X.Q., Zhang, J.J. & Zhang, L. The effect of La_2O_3 in Tm^{3+} -doped germanate-tellurite glasses for ~ 2 μm emission. *Sci. Rep.* **4**, 5256; DOI:10.1038/srep05256 (2014).



This work is licensed under a Creative Commons Attribution-NonCommercial-ShareAlike 4.0 International License. The images or other third party material in this article are included in the article's Creative Commons license, unless indicated otherwise in the credit line; if the material is not included under the Creative Commons license, users will need to obtain permission from the license holder in order to reproduce the material. To view a copy of this license, visit <http://creativecommons.org/licenses/by-nc-sa/4.0/>